CONTRIBUTION FROM THE SCIENTIFIC LABORATORY,
FORD MOTOR COMPANY, DEARBORN, MICHIGAN 48121

A Molecular Orbital Study of Vibronic Interactions in the Hexachlorocuprate(II) Complex

BY L. L. LOHR, JR.

Received May 23, 1967

The semiempirical LCAO-MO method is applied to the complex $CuCl_4^{4-}$, yielding electronic energies and wave functions useful in describing both the static and the dynamic aspects of the Jahn–Teller effect in this system. Electronic g values are calculated as a function of the molecular geometry and compared to those obtained from epr studies of Cu(II) in NaCl and $CdCl_2$. Vibrational energies are computed for the dynamic angular component of the e_g stretching mode, leading to a comparison of theoretical and experimental barriers to conversion between equivalent tetragonally elongated structures. Vibronic optical transition probabilities are calculated in detail, taking into account all nine odd-parity modes of a six-coordinated complex and using theoretical values for all harmonic oscillator force constants.

Introduction

Almost 30 years ago, Van Vleck considered[1] the coupling between the fourfold degenerate ^2E_g electronic ground state of an octahedral Cu(II) complex and the e_g vibrational mode, and showed that to a first approximation there would be a continuous series of nuclear configurations having the same electronic energy. These configurations are in general of only D_{2h} symmetry, with three different copper–ligand bond lengths, but there are certain configurations of D_{4h} symmetry, having only two different copper–ligand bond lengths. These higher symmetry configurations, corresponding to tetragonally elongated or compressed octahedra, represent extrema in the electronic energy when cubic terms are included[2] in an expansion of the energy in a power series in the nuclear coordinates.

Experimental evidence for three equivalent tetragonally elongated configurations separated by a small energy barrier comes from electron paramagnetic resonance (epr) studies of Cu(II) in single crystals of $ZnSiF_6 \cdot 6H_2O$,[3] $Mg_3La_2(NO_3)_{12} \cdot 24D_2O$,[3] MgO,[4,5] $CdCl_2$,[6] and, more recently, NaCl.[7,8] In each case, the epr spectrum at very low temperatures is that of a six-coordinated Cu(II) ion "frozen" into one of its minima, while at higher temperatures, ranging from 4°K for MgO to 95°K for NaCl, there is a transition to a spectrum that represents an average over the possible configurations. This nonrigid behavior is sometimes called the dynamic Jahn–Teller effect, although the dynamic behavior is not in the Jahn–Teller[9] active radial coordinate R, but is only in the angular coordinate α, where the nuclear coordinates α and R are a polar coordinate representation[1] of the two components of the e_g stretching mode. This dynamic behavior is in contrast to the dynamic Jahn–Teller effect in the vibrational spectra[10] of the heavy-metal hexafluorides, in which there is evidence for a significant breakdown of the Born–Oppenheimer approximation. This approximation[11] assumes that the nuclear motions are sufficiently slow that the total wave function $\Psi_{e,n}$ of the system may be factored into an electronic part ψ_e, depending parametrically on the instantaneous nuclear coordinates Q, as well as on the electronic coordinates q, and a nuclear part φ_n described by a set of vibrational quantum numbers v

$$\Psi_{e,n} = \psi_e(q, Q)\varphi(Q, v) \qquad (1)$$

By the term "Born–Oppenheimer," we shall always mean the above unrestricted factorization, rather than the restricted version in which $\psi_e(q, Q)$ is replaced by $\psi_e(q, Q_0)$, where Q_0 denotes the equilibrium nuclear configuration.

Electronic Energies and the Jahn–Teller Effect

The semiempirical LCAO–MO (linear combinations of atomic orbitals–molecular orbital) scheme, sometimes called the Wolfsberg–Helmholz[12] or extended Hückel[13] method, has provided[14] some very useful approximations to the electronic wave function $\psi_e(q, Q)$ and the associated total electronic energy $E_e(Q)$ for the Jahn–Teller systems VCl_4 and $CuCl_4^{2-}$. In the case of VCl_4, the scheme predicted a negligible static distortion, in contrast to the results[15] of a crystal-field approach. A more refined MO calculation[16] on VCl_4 also predicts little distortion.[17] For $CuCl_4^{2-}$, the method yielded electronic spectral predictions verified by experiment[18]

(1) J. H. Van Vleck, *J. Chem. Phys.*, **7**, 72 (1939); also see H. C. Longuet-Higgins, U. Öpik, M. H. L. Pryce, and R. A. Sack, *Proc. Roy. Soc.* (London), **A244**, 1 (1958).
(2) U. Öpik and M. H. L. Pryce, *ibid.*, **A238**, 425 (1956).
(3) B. Bleaney, K. D. Bowers, and R. J. Trenam, *ibid.*, **A228**, 157 (1955).
(4) J. W. Orton, P. Auzins, J. H. E. Griffiths, and J. E. Wertz, *Proc. Phys. Soc.* (London), **78**, 554 (1961).
(5) R. E. Coffman, *Phys. Letters*, **19**, 475 (1965); **21**, 381 (1965).
(6) J. H. M. Thornley, B. W. Mangum, J. H. E. Griffiths, and J. Owen, *Proc. Phys. Soc.* (London), **78**, 1263 (1961); for epr of Cu(II) in AgCl, see R. F. Tucker, Jr., *Phys. Rev.*, **112**, 725 (1958).
(7) R. Borcherts, H. Kanzaki, and H. Abe, Abstracts, International Symposium on Color Centers in Alkali Halides, University of Illinois, Urbana, Ill., Oct 1965.
(8) R. H. Borcherts, H. Kanzaki, and H. Abe, submitted for publication.
(9) H. A. Jahn and E. Teller, *Proc. Roy. Soc.* (London), **161**, 200 (1937).
(10) B. Weinstock and G. Goodman, *Advan. Chem. Phys.*, **9**, 169 (1965).
(11) M. Born and R. Oppenheimer, *Ann. Physik*, **84**, 457 (1927).
(12) M. Wolfsberg and L. Helmholz, *J. Chem. Phys.*, **20**, 837 (1952).
(13) R. Hoffmann and W. N. Lipscomb, *ibid.*, **36**, 2179, 3489 (1962); **37**, 2872 (1962).
(14) L. L. Lohr, Jr., and W. N. Lipscomb, *Inorg. Chem.*, **2**, 911 (1963).
(15) C. J. Ballhausen and A. D. Liehr, *Acta Chem. Scand.*, **15**, 775 (1961).
(16) C. J. Ballhausen and J. de Heer, *J. Chem. Phys.*, **43**, 4304 (1965).
(17) Y. Morino and H. Uehara, *ibid.*, **45**, 4543 (1966).
(18) J. Ferguson, *ibid.*, **40**, 3406 (1964); also see M. Sharnoff and C. W. Reimann, *ibid.*, **46**, 2634 (1967).

and electronic wave functions useful in the analysis of the epr spectrum.[19]

Recent epr studies[7,8] of Cu(II) dissolved in single crystals of NaCl have indicated the importance of studying the hexachlorocuprate(II) complex, $CuCl_6^{4-}$, formed when a Cu(II) ion occupies an Na site in NaCl. Applying the LCAO–MO scheme[20] to $CuCl_6^{4-}$, 57 valence electrons are assumed to occupy 29 MO's constructed from Cl(3s, 3p) and Cu(3d) Slater-type[21] atomic orbitals (AO's). Higher energy AO's, such as Cu(4s, 4p), may be included in the basis set to improve the shape of the MO's, bringing the total number of AO's to 33. There are uncertainties in the choice of both the Slater exponents and of the so-called Coulomb integrals, which are the diagonal elements of the undefined one-electron Hamiltonian, but for simplicity all parameters needed for $CuCl_6^{4-}$ were chosen as the values used[14] earlier for $CuCl_4^{2-}$. The geometric-mean bond energy recipe was used as before,[22,23] with the total electronic energy $E_e(Q)$ approximated[24] as

$$E_e(Q) = \sum_j n_j \lambda_j(Q) \qquad (2)$$

where n_j is the occupation number (0, 1, or 2) of the jth MO, and λ_j is the jth root of the LCAO–MO secular equation.

The nuclear coordinates to be considered here are the totally symmetric stretch (a_{1g}) and the Jahn–Teller active doubly degenerate stretch (e_g). In addition, all of the odd-parity deformations, both bending (t_{1u} and t_{2u}) and stretching (t_{1u}), are needed for the calculation of vibronic optical transition probabilities. While calculations for the neutral molecule VCl_4 yielded[14] a deep minimum at a V–Cl distance of 1.75 A, E_e for the highly charged complex $CuCl_6^{4-}$, assumed octahedral, has no minimum and, in fact, falls steeply as the Cu–Cl distance increases. If E_e at a Cu–Cl length of 2.4 A is taken to be zero, E_e is +8.39 ev at 2.2 A and −3.47 ev at 2.6 A. However, the method does describe the one-electron properties of the complex as a function of the bond distance. Figure 1 gives both the cubic crystal-field splitting parameter Δ, defined as the difference between the energies of the e_g and the t_{2g} mostly-3d MO's, and the fraction f of 3d character in each of these MO's. The fraction f_{ij} of the ith AO in the jth is defined[25] as

$$f_{ij} = \sum_k C_{ij} C_{kj} S_{ik} \qquad (3)$$

where C_{ij} and C_{kj} are the coefficients in the jth MO of the ith and kth AO's, respectively, and S_{ik} is the overlap of these AO's. Thus, for a Cu–Cl length of 2.4 A, Δ is 2.0 ev (16,100 cm^{-1}), while the e_g and t_{2g} MO's have about 77 and 95% 3d character, respectively.

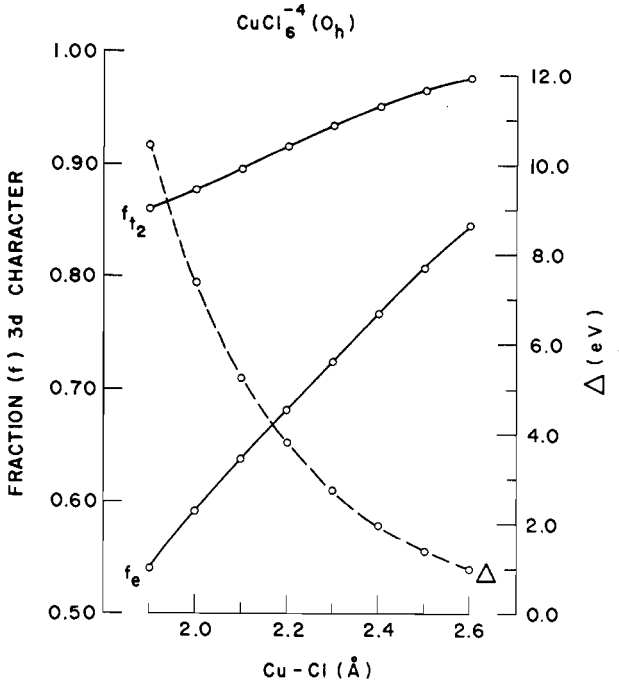

Figure 1.—Fractions of 3d character (solid lines) in the mostly-3d e_g and t_{2g} MO's for an octahedral $CuCl_6^{4-}$ complex and the energy difference Δ between the MO's (dashed lines), both as a function of the Cu–Cl distance.

In order to compute $E_e(Q)$, where Q denotes the e_g mode, a choice had to be made of the average distance[26] of the six Cu–Cl bonds, this average being kept constant for displacements along either the tetragonal or the orthorhombic components of the mode. A choice of 2.4 A corresponds roughly to the average Cu–Cl bond length in $CsCuCl_3$[27] (four bonds of 2.30 A, two of 2.65 A), $CuCl_2$[28] (four bonds of 2.30 A, two of 2.95 A), and $(NH_4)_2CuCl_4$[29] (two bonds of 2.30 A, two of 2.33 A, two of 2.79 A). The two lattices in which the epr spectrum of $CuCl_5^{4-}$ has been studied, NaCl[7,8] and $CdCl_2$,[6] have metal–ligand separations[30] of 2.81 and 2.65 A, respectively. While the average Cu–Cl distance associated with a Cu impurity in these lattices is uncertain, it is probably not greater than 2.6 A.

Figure 2 shows the energies of the ground state and those excited states formed by exciting one electron from the filled mostly-3d MO's into the singly occupied mostly-3d ($x^2 - y^2$) MO, while Figure 3 shows the corresponding fractions of 3d character (eq 3) in these MO's. Positive displacement for the two axial ligands corresponds to tetragonal elongation; negative, to tetragonal compression. In each case the displacement of the four equatorial ligands is minus half that of the axial ligands. Ground-state minima occur for axial displacements of ±0.15 A, with energies of 0.295 ev (elongated) and 0.290 ev (compressed), below the octahedral energy. The small difference of 0.005 ev,

(19) M. Sharnoff, *J. Chem. Phys.*, **41**, 2203 (1964); **42**, 3383 (1965).
(20) For LCAO–MO studies of CuF_6^{4-}, see ref 14 and H. Johansen and C. J. Ballhausen, *Mol. Phys.*, **10**, 175 (1966); also C. J. Ballhausen and H. Johansen, *ibid.*, **10**, 183 (1966).
(21) J. C. Slater, *Phys. Rev.*, **36**, 57 (1930).
(22) L. L. Lohr, Jr., *J. Chem. Phys.*, **45**, 3611 (1966).
(23) C. J. Ballhausen and H. B. Gray, *Inorg. Chem.*, **1**, 111 (1962).
(24) For a discussion of this approximation, see L. C. Allen and J. D. Russell, *J. Chem. Phys.*, **46**, 1029 (1967).
(25) R. S. Mulliken, *ibid.*, **23**, 1833 (1955).
(26) For a review of Cu–Cl distances, see L. E. Orgel and J. D. Dunitz, *Nature*, **179**, 462 (1957).
(27) A. F. Wells, *J. Chem. Soc.*, 1662 (1947).
(28) A. F. Wells, *ibid.*, 1670 (1947).
(29) R. D. Willett, *J. Chem. Phys.*, **41**, 2243 (1964).
(30) R. W. G. Wyckoff, "Crystal Structures," Vol. I, Interscience Publishers, Inc., New York, N. Y., 1960.

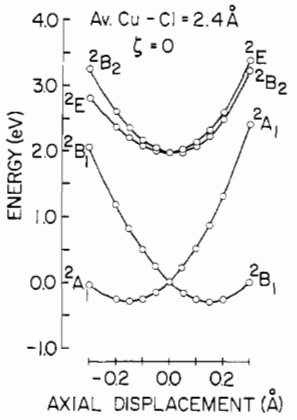

Figure 2.—Total energy curves for ground and excited states of $CuCl_6^{4-}$ as a function of the Jahn–Teller active tetragonal distortion, with positive axial displacement for elongation and negative for compression. States are labeled by their D_4 representation symbols; all are g representations of D_{4h}.

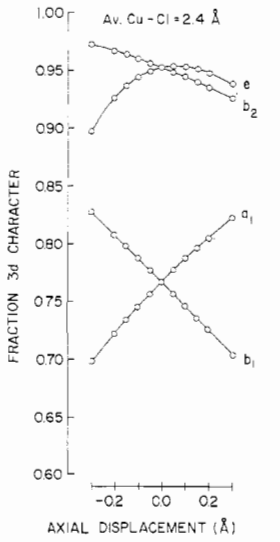

Figure 3.—Fractions of 3d character in the mostly-3d MO's as a function of the tetragonal distortion of Figure 2.

or 40 cm^{-1}, between the two types of minima corresponds to the barrier separating equivalent elongated minima, for the compressed geometry is a saddle point, having a maximum energy in the angular coördinate α and a minimum in the radial coordinate. When the average Cu–Cl length is decreased to 2.2 A, Δ is increased from 2.0 to 3.8 ev, with the energy decrease upon tetragonal elongation increasing to 0.515 ev. The barrier is also increased, rising to 0.025 ev, or 186 cm^{-1}. The minima again occur for axial displacements of ± 0.15 A.

It is generally assumed[31] that the angular barrier is adequately represented by a potential energy V of the form

$$V(\alpha) = [1 - \cos(3\alpha)]B/2 \qquad (4)$$

even though the only symmetry requirement is that V be periodic in 3α. In any case, V is zero for the three tetragonally elongated structures at $\alpha = 0$, $2\pi/3$, and $4\pi/3$, while V equals the barrier height B for the compressed structures at $\alpha = \pi/3$, π, and $5\pi/3$. Indeed, the computation of $E_e(\alpha)$, which is equivalent to $V(\alpha)$, at increments of $\pi/36$ between $\alpha = 0$ and $\alpha = \pi/3$, assuming an average Cu–Cl length of 2.2 A, shows a maximum deviation of only 1.5% below V of eq 4 at $\alpha = \pi/6$.

The computed value of B is a very small fraction of the total electronic energy and has only semiquantitative significance. While the magnitude of 40 cm^{-1} for an average Cu–Cl distance of 2.4 A is shown in the Nuclear Dynamics section to be only one-seventh of the experimental value, the sign is correct. The reason that the LCAO–MO method yields a slightly lower energy for the elongated structure relative to the compressed[32] is that the tetragonal distortion about the z axis of the complex brings about a mixing of the Cu(4s) AO into the MO that is largely Cu(3d, $3z^2 - r^2$). If the complex is elongated, there are two electrons in this MO, while there is only one if compressed.[33] Thus that structure is favored which can take advantage twice, rather than just once, of a flexibility in the shape of this MO which is not available to the MO that is largely Cu(3d, $x^2 - y^2$). Indeed, calculations in which Cu(4s, 4p) were excluded from the basis set yield a negative barrier of about 0.020 ev when the average Cu–Cl distance is 2.4 A. It should be noted that the electrostatic energy of Cu^{2+} and Cl^- point charges is 0.014 ev less for a compressed structure (two Cu–Cl of 2.25 A, four of 2.475 A) than for an elongated structure (two Cu–Cl of 2.55 A, four of 2.325 A).

The results of this portion of the study are summarized in Figure 4, showing the computed E_e values as contours in the polar coordinates α and R, where R is identical with the axial ligand displacement of Figures 2 and 3. The contour for energy equal to the barrier is 0.04 A wide along the elongated radial directions, narrowing, of course, to zero width at the saddle points in the compressed directions.

If we approximate the radial potential of Figure 2 as a harmonic oscillator[34] in one dimension about the minima, we compute a vibrational frequency of 260 cm^{-1}, corresponding to a zero-point energy of 130 cm^{-1}, and a root-mean-square (rms) displacement of $0.035(v + 1/2)^{1/2}$ A, where v is the vibrational quantum number. These numbers compare with the Jahn–Teller stabilization of 0.295 ev, or 2380 cm^{-1}, for a radial displacement of 0.15 A, to indicate that for $CuCl_6^{4-}$ there is a Jahn–Teller effect that is essentially static in R, even though the molecule may be nonrigid with respect to α.

The five mostly-3d MO's for the tetragonally elongated minimum with Cl nuclei located at ± 2.325 A on the x

(31) M. C. M. O'Brien, *Proc. Roy. Soc.* (London), **A281**, 323 (1964).

(32) A compressed structure is favored for CuF_6^{4-} in the pure salt K_2CuF_4 [K. Knox, *J. Chem. Phys.*, **30**, 991 (1959)], but not CuF_2 [C. Billy and H. M. Haendler, *J. Am. Chem. Soc.*, **79**, 1049 (1957)]. The compressed structure reported for $KCuF_3$ [A. J. Edwards and R. D. Peacock, *J. Chem. Soc.*, 4126 (1959)] appears to be incorrect [A. Okazaki and Y. Suemune, *J. Phys. Soc. Japan*, **16**, 176 (1961)].

(33) For the first *excited* state of Figure 2, the compressed structure ($^2B_{1g}$) lies 0.057 ev, or 460 cm^{-1}, below the elongated structure ($^2A_{1g}$).

(34) H. Eyring, J. Walter, and G. E. Kimball, "Quantum Chemistry," John Wiley and Sons, Inc., New York, N. Y., 1944, pp 75–79; the effective mass is 3 times the Cl mass (see ref 31).

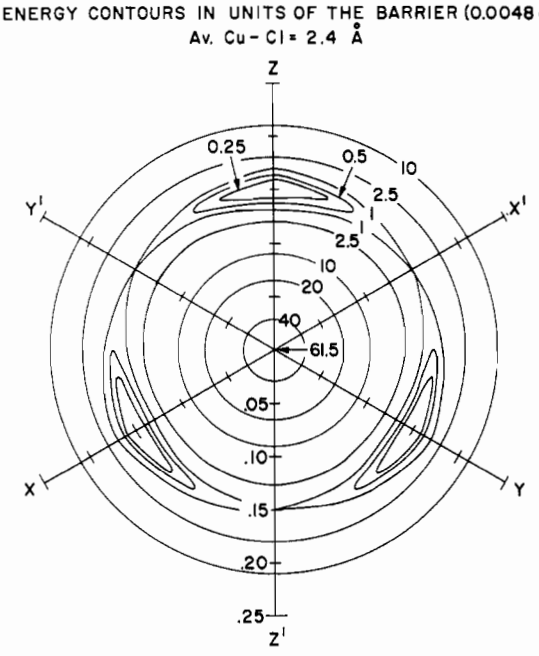

Figure 4.—Energy contours for the electronic ground state in the α, R space for the $CuCl_6^{4-}$ complex. Minima occur for R = 0.15 A along X, Y, and Z, with saddle points at the same distance along X', Y', and Z'. The energy is taken to be zero at the tetragonal minima, unlike the choice in Figure 2, where the octahedral configuration was given zero energy. Here the octahedral configuration has an energy of 61.5 times the barrier, or +0.295 ev.

axis, ±2.325 A on the y axis, and ±2.550 A on the z axis are given in Table I as the coefficients of the Slater-type AO basis set, with exponents of 2.03 for Cl(3s, 3p), 1.35 for Cu(4s, 4p), and 2.41 for Cu(3d).

TABLE I

EIGENVECTORS FOR THE MOSTLY-3d MO's[a,b]

AO[c,d]	b_{1g}	a_{1g}	b_{2g}	e_g	
s(1, 2)	0.1284	−0.0432	0.0	0.0	0.0
s(3, 4)	−0.1284	−0.0432	0.0	0.0	0.0
s(5, 6)	0.0	0.1172	0.0	0.0	0.0
x(1, 2)	∓0.3052	±0.1490	0.0	0.0	0.0
x(3, 4)	0.0	0.0	±0.1438	0.0	0.0
x(5, 6)	0.0	0.0	0.0	0.0	∓0.0795
y(1, 2)	0.0	0.0	±0.1438	0.0	0.0
y(3, 4)	±0.3052	±0.1490	0.0	0.0	0.0
y(5, 6)	0.0	0.0	0.0	±0.0795	0.0
z(1, 2)	0.0	0.0	0.0	0.0	∓0.1652
z(3, 4)	0.0	0.0	0.0	±0.1652	0.0
z(5, 6)	0.0	∓0.3025	0.0	0.0	0.0
4s(Cu)	0.0	−0.0594	0.0	0.0	0.0
$3z^2 - r^2$(Cu)	0.0	−0.9446	0.0	0.0	0.0
$x^2 - y^2$(Cu)	−0.9393	0.0	0.0	0.0	0.0
xy(Cu)	0.0	0.0	−0.9820	0.0	0.0
xz(Cu)	0.0	0.0	0.0	0.0	0.9841
yz(Cu)	0.0	0.0	0.0	−0.9841	0.0

[a] MO's labeled by their D_{4h} representation symbols. [b] One-electron eigenvalues are −7.13, −8.30, −9.66, −9.75, and −9.75 ev, respectively. [c] The symbol 3s(1, 2) denotes the 3s AO for Cl_1 and Cl_2, respectively. [d] Coordinates are $Cl_{1,2}$ at ±2.325 A on the x axis, $Cl_{3,4}$ at ±2.325 A on the y axis, and $Cl_{5,6}$ at ±2.55 A on the z axis, with Cu at the origin.

Spin–Orbit Coupling and g Values

The epr evidence[3-8] for the dynamic behavior of six-coordinated Cu(II) complexes consists of drastic changes in the observed g values with temperature. At low temperatures the spectrum is described by $g_{||}$ and $g_\perp$, for the magnetic fields parallel and perpendicular to the fourfold axis of the complex, while at higher temperatures, about 95°K for Cu(II) in NaCl,[7,8] a single epr line is observed with a g value equal to $(g_{||} + 2g_\perp)/3$. The theory[35] of these g values, relating them to a spin–orbit parameter and to energy splittings of the 3d orbitals, is particularly simple if the spin–orbit and orbital angular momentum matrix elements are computed for atomic orbitals. The energy splittings are usually taken as parameters or fitted to optical spectra. However, the LCAO–MO method provides orbital splittings directly as a function of the nuclear coordinates, permitting computation of both $g_{||}$ and $g_\perp$ in terms of these coordinates (Figure 5). These values are obtained by diagonalizing both the spin–orbit and Zeeman energies within the ten-state basis having "crystal-field" energies as shown in Figure 2. For simplicity, the spin–orbit parameter ζ_{3d} was taken to equal 826 cm^{-1} or 0.102 ev, the spectroscopic free-ion value,[36] and the one-center approximation, with all orbital angular momentum (**L**) matrix elements having only central-atom contributions, was made. Values are shown both for the electronic ground state ($^2B_{1g}$ for positive axial displacement, $^2A_{1g}$ for negative displacement) and for the upper Jahn–Teller half-state ($^2A_{1g}$ for positive displacement, $^2B_{1g}$ for negative). The dashed lines for $g_\perp$ near zero displacement indicate the region of the orbital quantization problem; if the complex has O_h symmetry, the electronic state is ^2E_g, with the two g values shown on the two $g_{||}$ curves (1.995 and 2.396). A magnetic field along the x axis, say, causes the orbital states to become $|3x^2 - r^2\rangle$ and $|z^2 - y^2\rangle$, with g values identical with those for the field along y or z. The quantity $g_\perp$ only has meaning when the orbital states are "locked-in" as $|3z^2 - r^2\rangle$ and $|x^2 - y^2\rangle$ by a tetragonal distortion along z that produces a splitting large compared to

$$\frac{\langle 3z^2 - r^2|\beta H_x L_x|yz\rangle\langle yz|\beta H_x L_x|x^2 - y^2\rangle}{\Delta} = \frac{3^{1/2}(\beta H_x)^2}{\Delta} \quad (5)$$

where β is the Bohr magneton, H_x is the x component of the magnetic field, and Δ is the cubic splitting. For a magnetic field of 3000 gauss and Δ of 16,000 cm^{-1}, the above matrix element equals only 2.1×10^{-6} cm^{-1}! Very little tetragonal splitting is required to quench this effect, so that the $g_\perp$ curves of Figure 5 could have been extended along the dashed lines very close to zero axial displacement.

The g values shown in Figure 3 for $CuCl_6^{4-}$ at the elongated minimum of Figure 2 are 2.314 for $g_{||}$ and 2.074 for $g_\perp$, close to experimental values[6] for Cu(II) in $CdCl_2$ of 2.339 ± 0.002 for $g_{||}$ and 2.070 ± 0.002 for $g_\perp$. For Cu(II) in NaCl,[7,8] $g_{||}$ is larger (2.37 ± 0.01), while $g_\perp$ is the same (2.07 ± 0.01). The simplest perturbation theory, which assumes that the cubic splitting is

(35) A. Abragam and M. H. L. Pryce, *Proc. Phys. Soc.* (London), **A63**, 409 (1950).

(36) C. E. Moore, National Bureau of Standards Circular No. 467, Vol. II, U. S. Government Printing Office, Washington, D. C., 1952.

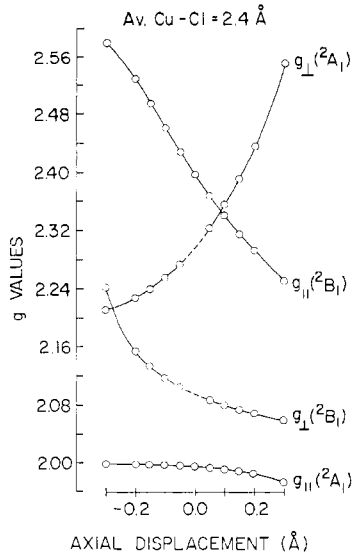

Figure 5.—Values of $g_{||}$ and $g_\perp$ for both tetragonal components of the ^2E_g octahedral state. See text for discussion of the significance of the dashed portions of the $g_\perp$ curves.

very large relative to the tetragonal splitting of the $^2T_{2g}$ excited state, gives a ratio of the orbital parts of $g_{||}$ and $g_\perp$ of exactly 4, while the ratio from Figure 3 is 4.38 at the tetragonal minimum and is an insensitive function of the radial coordinate (the ratio goes from 4.34 to 4.39 as the displacement increases from 0.1 to 0.2 A). However, the experimental ratios for Cu(II) in NaCl and $CdCl_2$ are 5.28 and 4.92, respectively.

Perturbation expressions for $g_{||}$ and $g_\perp$ are

$$g_{||} = g_z = 2.0023 + \frac{4\langle ^2B_{1g}, {}^1/_2|H_{so}|^2B_{2g}, {}^1/_2\rangle\langle ^2B_{2g}, {}^1/_2|L_z|^2B_{1g}, {}^1/_2\rangle}{E(^2B_{2g}) - E(^2B_{1g})}$$

$$g_\perp = g_x = 2.0023 + \frac{4\langle ^2B_{1g}, {}^1/_2|H_{so}|^2E_g(yz), -{}^1/_2\rangle\langle ^2E_g(yz), -{}^1/_2|L_x|^2B_{1g}, -{}^1/_2\rangle}{E(^2E_g) - E(^2B_{1g})} \quad (6)$$

where H_{so} is the one-electron spin–orbit coupling operator,[37] L_x and L_z are dimensionless components of the orbital angular momentum, $\pm{}^1/_2$ is the spin projection value, and yz denotes the orbital component of the degenerate ^2E state that contributes to g_x. If all matrix elements are evaluated using 3d AO's, rather than generalized MO's, then

$$\frac{g_{||} - 2.0023}{g_\perp - 2.0023} = 4\left[1 + \frac{E(^2E_g) - E(^2B_{2g})}{E(^2B_{2g}) - E(^2B_{1g})}\right] \quad (7)$$

that is, the above ratio is increased rapidly by an increase in the tetragonal splitting of the $^2T_{2g}$ term into ^2E_g and $^2B_{2g}$ terms. In fact, the g values for Cu(II) in NaCl can be fitted to perturbation formulas with a tetragonal splitting of 5750 cm^{-1}, together with a value of 17,850 cm^{-1} for $E(^2B_{2g}) - E(^2B_{1g})$ and the free-ion spin–orbit parameter of 826 cm^{-1}. Other fits of the values are possible when the matrix elements of H_{so} and **L** are permitted to differ from their purely-3d values, but perhaps more important here is an underestimation of the tetragonal splitting by the simple LCAO–MO method (only 760 cm^{-1} at the elongated minimum in Figure 2). Such a shortcoming would not be surprising, since it represents an underestimation of π antibonding relative to σ antibonding, a feature that is inherent in the method as long as the resonance integral between two AO's is assumed[22,23] to be proportional to their overlap, but otherwise independent of their relative orientation.

Another description of Cu(II) in NaCl would be one with an average Cu–Cl distance somewhat larger than 2.4 A. Increasing this separation to 2.5 A, Δ is reduced from 2.0 to 1.4 ev (Figure 1), bringing the excitation energies roughly into line with experimental values[38] for $CuCl_6^{4-}$ in $CsCuCl_3$ (average Cu–Cl of 2.42 A) of 1.46 ev for $^2B_{1g} \rightarrow {}^2E_g$, and 1.36 ev for $^2B_{1g} \rightarrow {}^2B_{2g}$, or an experimental tetragonal splitting of only 0.1 ev = 800 cm^{-1}. The orbital contributions to g will then be far too large unless substantial reduction of the spin–orbit and/or orbital angular momentum matrix elements by covalency is invoked. Such corrections can be estimated from the coefficients of Table I or from the fractions of 3d character in Figures 1 and 3, yielding over-all reduction factors of 0.69 and 0.74 for average Cu–Cl distances of 2.4 and 2.5 A, respectively. Since the energy denominators in the $g_{||}$ and $g_\perp$ expressions will have values at the latter distance of about $^{1.4}/_{2.0}$, or 0.7 times the values at the shorter distance, g values computed at the larger distance with consideration of covalency effects will nearly equal g values at the shorter distance without this consideration.

Finally, the effect of spin–orbit coupling on the potential curves for the tetragonal distortion is shown in Figure 6, where the states are labeled by their spinor representations for the group D_4^*. If the complex is octahedral, the second-order depression of the ground state is only 62 cm^{-1}, while the excited $^2T_{2g}$ state is split by 1300 cm^{-1}, slightly larger than the first-order splitting of $3\zeta_{3d}/2$, or 1240 cm^{-1}. The few per cent decrease in the barrier height B from the value without spin–orbit coupling is unimportant.

Nuclear Dynamics and the Epr Spectrum

The kinetic energy T_n of the six Cl nuclei in the e_g vibrational mode is represented[31] in polar coordinates by the operator

$$T_n = \frac{-\hbar^2}{2M}\left[\frac{\partial^2}{\partial R^2} + \frac{1}{R}\frac{\partial}{\partial \alpha} + \frac{1}{R^2}\frac{\partial^2}{\partial \alpha^2}\right] \quad (8)$$

where the effective mass M equals 3 times the Cl mass. As the Cl^{35} and Cl^{37} isotopes have natural abundances of approximately 75 and 25%, respectively, only 17.8% of the complexes are $Cu(Cl^{35})_6^{4-}$. The most abundant species, 35.6%, is $Cu(Cl^{35})_5(Cl^{37})^{4-}$, while there are 23.8% *cis*-$Cu(Cl^{35})_4(Cl^{37})_2^{4-}$ and 5.9% *trans*-$Cu(Cl^{35})_4$-

(37) J. S. Griffith, "The Theory of Transition Metal Ions," Cambridge University Press, New York, N. Y., 1961, pp 106–113.

(38) P. Day, *Proc. Chem. Soc.*, 18 (1964).

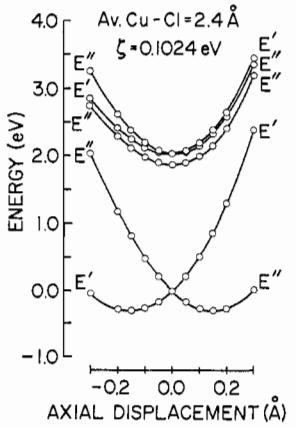

Figure 6.—Total energy curves as in Figure 2 but with spin–orbit coupling included. States are labeled by their D_4^* (spinor group) representation symbols.

$(Cl^{37})_2^{4-}$. The remaining complexes contain three or more Cl^{37} nuclei, but only 0.025% have six Cl^{37} nuclei. Thus for 82.2% of the complexes there will be small correction terms to the nuclear kinetic energy (eq 8) that will explicitly contain the coordinate α, but which will be ignored.

If the potential V is a function of R only, as it nearly is for small barriers, the vibrational wave function φ_n is a product of a radial function $\varphi_R(R)$ and an angular function $\varphi_\alpha(\alpha)$. Since the Born–Oppenheimer ground-state electronic function[1,35] for the unpaired electron is

$$\psi_e(\alpha) = \cos(\alpha/2)|x^2 - y^2\rangle + \sin(\alpha/2)|3z^2 - r^2\rangle \quad (9)$$

where $\psi_e(2\pi) = -\psi_e(0)$, the function $\varphi_\alpha(\alpha)$ must satisfy $\varphi_\alpha(2\pi) = -\varphi_\alpha(0)$, so that the total electronic–nuclear wave function is unchanged upon increasing α by 2π, which is the smallest increment in α which returns the nuclear configuration to its initial form. Acceptable[31] angular functions are

$$\varphi_\alpha(\alpha) = (2\pi)^{-1/2}e^{im\alpha};\ m = \pm 1/2,\ \pm 3/2, \text{ etc.} \quad (10)$$

with energies

$$\Lambda_m = \frac{\hbar^2}{2MR^2}m^2 = Gm^2 \quad (11)$$

where $\hbar$ is Planck's constant divided by 2π. If R is 0.15 A, G equals 7.05 cm^{-1}. It should be noted that although $\varphi_\alpha(\alpha)$ takes the form of the function for a particle rotating in a plane about a point, the vibrational angular momentum is actually zero, as each Cl moves only along its bond axis.

The radial function $\varphi_R(R)$ will be dependent upon the angular quantum number m unless the Jahn–Teller stabilization is large, in which case complete separation of the angular and radial Schrödinger equations is approached. A harmonic oscillator description of the radial motion based on the potential curves of Figure 2 was given at the end of the Electronic Energies section.

In the presence of the periodic potential (eq 4), the angular wave functions can, of course, be expressed as linear combinations of basis functions of the type given in eq 10, with the selection rule $\Delta m = \pm 3$ governing the mixing. For sufficiently large B, these functions, like the radial functions, may be found using the harmonic approximation. If $B = 100$ cm^{-1}, a frequency of 77 cm^{-1} is computed, with an rms angular displacement of $0.42(v + 1/2)^{1/2}$ radians, which is 17° for $v = 0$. Using the computed value for B of 40 cm^{-1}, the frequency is 49 cm^{-1}, larger than B, and the rms angular displacement for $v = 0$ is 21°. The harmonic force constant K is taken here to be $9B/2$, matching the curvature of eq 4 at $\alpha = 0$.

If the ground-state vibrational function centered about $\alpha = 0$ is

$$\varphi_n = (c/\pi)^{1/4}e^{-c\alpha^2/2} \quad (12)$$

where

$$c = (MR^2K)^{1/2}/\hbar = 3R(3m_{Cl}B/2)^{1/2}/\hbar \quad (13)$$

the overlap S_n of this function with one centered about $\alpha = 2\pi/3$ is

$$S_n = e^{-c(\pi/3)^2} \quad (14)$$

This overlap is 2.0×10^{-2} for B of 40 cm^{-1}, falls to 2.0×10^{-3} for B of 100 cm^{-1}, and essentially vanishes (2.0×10^{-9}) for B of 1000 cm^{-1}. In the theory of O'Brien,[31] the epr observation of "localized" states at low temperatures implies that the off-diagonal Zeeman matrix element between the ground-state vibrational doublet and the first excited vibrational singlet is comparable to, or greater than, the "inversion" separation[39,40] of these levels, which are the stationary states of the system with the periodic potential, but without the magnetic field. Applying this theory, the magnitude of this separation can be no greater than $(1 + 2^{1/2})\cdot(g_\parallel - g_\perp)\beta H/3$, or 0.034 cm^{-1} for a 3000-gauss field and $g_\parallel$, $g_\perp$ values taken from the epr spectrum[7,8] of Cu(II) in NaCl.

If H_{aa} and H_{ab} are the diagonal and off-diagonal elements of a Hamiltonian consisting of eq 4 plus the last term of eq 8 with respect to the functions of eq 12, the roots of the secular equation representing the cyclic interaction of three equivalent wells centered about $\alpha = 0$ and $\pm 2\pi/3$ are

$$\lambda_1 = \lambda_2 = \frac{H_{aa} + H_{ab}}{1 + S_n} \equiv \lambda(e) \quad (15)$$

and

$$\lambda_3 = \frac{H_{aa} - 2H_{ab}}{1 - 2S_n} \equiv \lambda(a)$$

These values, resembling simple MO energies for equilaterally triangular H_3, but with signs reversed, reflect the use of properly symmetrized[31] eigenstates that, like the functions in eq 10, change sign on increasing α by 2π. The splitting between the upper nondegenerate vibrational state and the lower doublet is

$$\lambda(a) - \lambda(e) = \frac{-3(H_{ab} - S_nH_{aa})}{(1 + S_n)(1 - 2S_n)} \quad (16)$$

(39) I. B. Bersuker, *Zh. Eksperim. i Teor. Fiz.*, **43**, 1315 (1962); **44**, 1239 (1963); *Soviet Phys. JETP*, **16**, 933 (1963); **17**, 836 (1963).

(40) I. B. Bersuker, S. S. Budnikov, B. G. Vekhter, and B. I. Chinik, *Fiz. Tverd. Tela*, **6**, 2583 (1964); *Soviet Phys.-Solid State*, **6**, 2059 (1965).

where

$$H_{nb} - S_n H_{aa} = S_n[-c^2G(\pi/3)^2 + Be^{-9/4c}] \quad (17)$$

B is the barrier, while G is the constant from eq 11. For barriers of 40, 100, 200, and 300 cm^{-1}, the splitting is 4.65, 1.08, 0.163, and 0.0322 cm^{-1}, respectively. Hence, the barrier is at least 300 cm^{-1} in height, or over seven times the 40-cm^{-1} LCAO–MO value for an average Cu–Cl distance of 2.4 A.

If the barrier is 300 cm^{-1}, the harmonic approximation to the potential yields a frequency of 133 cm^{-1} and an rms angular displacement of 13.0° in the ground vibrational state. The overlap of functions in adjacent wells is 2.4×10^{-5} for $v = 0$, but is -20.5 times greater for $v = 1$. In fact, the transition to a g-average spectrum at higher temperatures requires the occupation of vibrational states with separations from other states large relative to the off-diagonal Zeeman interactions, a condition satisfied for a temperature of 100°K with a barrier of the order of 300°K.

It is the symmetry properties forced on the vibrational functions by the symmetry of the electronic function (eq 9) that makes the vibrational ground state doubly degenerate, not the negative overlap of electronic wave functions for adjacent wells, as recently claimed.[41] While it is true that the overlap of $\psi_e(\alpha)$ with $\psi_e(\alpha')$ is $-1/2$ for $\alpha = 0$ and $\alpha' = 4\pi/3$, the overlap is $+1/2$ for the pairs $\alpha = 0$, $\alpha' = 2\pi/3$ and $\alpha = 2\pi/3$, $\alpha' = 4\pi/3$. However, this overlap does not enter the calculation of the interaction energy between adjacent wells at all if the unrestricted Born–Oppenheimer approximation is used (eq 1), for then α equals α', and the electronic overlap is simply unity.

It has been assumed here that both the electronic and vibrational properties of Cu(II) in NaCl can be adequately described in terms of the effective molecule $CuCl_6^{4-}$. While the electronic wave functions may indeed be essentially localized within a seven-atom complex, the vibrational functions may not be so localized. In fact, there is a large family of NaCl lattice modes all with e_g point-group symmetry with respect to a cation site, but with varying strengths of coupling to the ^2E_g electronic state of octahedrally coordinated Cu(II). However, all of the interesting quantum mechanics in the α coordinate still applies, as it is based on symmetry considerations, but the magnitudes of effects may vary from those expected for the complex $CuCl_6^{4-}$. In addition, the near-degeneracy of the lowest three α-vibrational levels of the complex may be destroyed by random crystal strains, stabilizing a particular crystal direction for the tetragonal axis of any given complex. If the strains are not too large, the high-temperature average g value may not differ enough from $(g_{\parallel} + 2g_{\perp})/3$ to distinguish strains from the Zeeman perturbations in O'Brien's theory[31] as the explanation for observing "frozen" distortions at low temperatures.

(41) U. T. Höchli and T. L. Estle, *Phys. Rev. Letters*, **18**, 128 (1967).

Vibronic Optical Transitions

Optical transitions between even-parity electronic states are another manifestation of electronic–vibrational coupling in transition metal complexes. The LCAO–MO method provides a conceptually simple way of computing the electric dipole intensities of these transitions, induced between the states of Figure 2 by coupling[42,43] to odd-parity vibration modes. The unrestricted Born–Oppenheimer approximation (eq 1) is used, letting Q denote one of the nine odd-parity modes. These modes span the representations t_{1u}, t_{1u}, and t_{2u} of the group O_h, the t_{2u} modes being purely bending, while the two t_{1u} sets are chosen[44] so that one set is also purely bending, while the other resembles the asymmetric stretch of a linear triatomic molecule, plus some bending of the remaining four bonds.

For the elongated D_{4h} complex, the nine modes will have six different frequencies and will transform like $a_{2u} + e_u$ (corresponding to t_{1u}) and $b_{2u} + e_u$ (corresponding to t_{2u}). Electronic wave functions $\psi_e(Q)$ are computed for a succession of both small and large displacements along each of the six coordinates described in Tables II and III. Electric dipole transition

TABLE II

COORDINATES FOR ODD-PARITY BENDING MODES

	x, A	y, A	z, A
	t_{1u} (a_{2u}) and t_{2u} (b_{2u}) Modes[a,b]		
$Cl_{1,2}$	$\pm 2.325 \cos\theta$	0	$2.325 \sin\theta$
$Cl_{3,4}$	0	$\pm 2.325 \cos\theta$	$2.325 \sin\theta$[c]
$Cl_{5,6}$	0	0	± 2.550
Cu	0	0	0
	t_{1u} (e_u) and t_{2u} (e_u) Modes		
$Cl_{1,2}$	$\pm 2.325 \cos\theta$	$2.325 \sin\theta$[c]	0
$Cl_{3,4}$	0	± 2.325	0
$Cl_{5,6}$	0	$2.550 \sin\theta'$[d]	$\pm 2.550 \cos\theta'$[d]
Cu	0	0	0

[a] D_{4h} representations are in parentheses. [b] For bends beginning with the tetragonally compressed minimum, replace 2.550 by 2.250 and 2.325 by 2.475, throughout. [c] Given for the t_{1u} mode; change sign for the t_{2u} mode. The shift of center of mass for t_{1u} is corrected for in the effective mass.[46] [d] The angle θ' is chosen so that the center of mass is unshifted in the t_{2u} mode; that is, $2.550 \sin\theta' = 2.325 \sin\theta$.

moments are then calculated[45] within the set of five mostly-3d MO's for each deformation, yielding moments that are odd functions of the displacement coordinates. For moderate displacements, these moments are very nearly proportional to the coordinate. For example, out-of-plane bending by 5° of the four equatorial Cl atoms along the b_{2u} component of the t_{2u} mode yields a z-polarized moment of -0.067 A be-

(42) G. Herzberg and E. Teller, *Z. Physik. Chem.*, **B21**, 410 (1933).
(43) A. D. Liehr, *Advan. Chem. Phys.*, **5**, 241 (1963).
(44) H. H. Claassen, *J. Chem. Phys.*, **30**, 968 (1959).
(45) The oscillator strengths are calculated in an approximation which assumes that all off-diagonal two-center matrix elements of the electric dipole operator **R** correspond to a vector directed to the midpoint of the two centers (exact for AO's identical except for position). This approximation, which enables the transition moments (off-diagonal matrix elements of **R**) to be expressed in terms of the MO coefficients and the AO overlap integrals, is identical with that made in the population analysis scheme used to obtain atomic charges, which divides the overlap contributions equally between the two AO's involved.

TABLE III

COORDINATES FOR ODD-PARITY STRETCHING MODES

	x, A	y, A	z, A
		t_{1u} (a_{2u}) Mode[a,b]	
$Cl_{1,2}$	±2.325	0	0
$Cl_{3,4}$	0	±2.325	0
$Cl_{5,6}$	0	0	$\pm 2.550 - 2.325\delta$
Cu	0	0	$2.325(2m_{Cl}/m_{Cu})\delta$[c]
		t_{1u} (e_u) Mode[a,b]	
$Cl_{1,2}$	±2.325	0	0
$Cl_{3,4}$	0	$\pm 2.325(1 \pm \delta)$	0
$Cl_{5,6}$	0	0	±2.550
Cu	0	$2.325(2m_{Cl}/m_{Cu})\delta$	0

[a] D_{4h} representations are in parentheses. [b] See footnote *b*, Table II. [c] m_{Cl} and m_{Cu} are the Cl and Cu masses, respectively.

f for polarized light propagating in a medium with all molecules identically oriented is given[47] by

$$f = \frac{4\pi m\nu}{\hbar}\mathbf{R}_{ik}^2 \qquad (18)$$

where m is the electron mass, ν is the frequency in sec^{-1}, and $\mathbf{R}_{ik}$ is the transition moment between states i and k. The f values in Tables IV and V may be combined to represent Cu(II) in NaCl, where there are three differently oriented complexes, yielding a value of 0.291×10^{-4} for the absorption from $^2B_{1g}$ to the Jahn–Teller half-state $^2A_{1g}$ and a value of 1.630×10^{-4} to the combined $^2B_{2g}$ and ^2E_g states. While the transition to $^2A_{1g}$ is essentially isotropic (0.328×10^{-4} for the electric vector $\mathbf{E}||z$, 0.273×10^{-4} for $\mathbf{E} \perp z$), the transition to $^2B_{2g}$, ^2E_g is highly polarized (0.027×10^{-4} for $\mathbf{E}||z$, 2.431 for $\mathbf{E} \perp z$, where z is the C_4 axis of a given complex).

TABLE IV

COMPUTED FREQUENCIES OF ODD-PARITY VIBRATIONAL MODES AND VIBRONIC INTENSITIES

Mode (O_h)	Mode (D_{4h})	Molecular symmetry	$A(1, z, 2)$[a,b]	$A(1, x, 4)$[c]	Force constant[d] × 10^{-4}, dynes cm^{-1}	Freq,[d] cm^{-1}	$f(^2B_g \longrightarrow {}^2A_{1g})$[e]	$f(^2B_{1g} \longrightarrow {}^2E_g(xz))$
t_{2u} (bend)	b_{2u}	D_{2d}	−0.333	0.227	12.2	120	0.328×10^{-4}	0.344×10^{-4}
t_{1u} (bend)	a_{2u}	C_{4v}	0	0.229	16.2	200	0	0.435×10^{-4}
t_{1u} (str)	a_{2u}	C_{4v}	0	−0.379	41.2	216	0	0.528×10^{-4}

[a] $A(i, j, k) \equiv \langle i(Q)|r_j|k(Q)\rangle/Q$ and is dimensionless. [b] The numbers 1, 2, 3, 4, and 5 denote those MO's which are primarily $x^2 - y^2$, $3z^2 - r^2$, xy, xz, and yz, respectively. [c] Equals $A(1, y, 5)$ for t_{2u}; change sign for t_{1u}. [d] Computed from LCAO–MO $E_e(Q)$, and are molecular, not bond, force constants. [e] Dimensionless oscillator strength.

TABLE V

COMPUTED FREQUENCIES OF ODD-PARITY VIBRATIONAL MODES AND VIBRONIC INTENSITIES[a]

Mode[b] (O_h)	$A(1, y, 2)$	$A(1, x, 3)$	$A(1, z, 5)$	Force constant × 10^{-4}, dynes cm^{-1}	Freq, cm^{-1}	$f(^2B_{1g} \longrightarrow {}^2A_{1g})$	$f(^2B_{1g} \longrightarrow {}^2B_{2g})$	$f(^2B_{1g} \longrightarrow {}^2E_g(yz))$
t_{2u} (bend)	−0.160	−0.241	0.017	16.2	138	0.660×10^{-5}	0.324×10^{-4}	0.167×10^{-6}
t_{1u} (bend)	−0.026	0.237	0.011	17.7	207	0.240×10^{-6}	0.430×10^{-4}	0.913×10^{-7}
t_{1u} (str)	0.384	−0.353	0.057	55.7	251	0.202×10^{-4}	0.370×10^{-4}	0.101×10^{-5}

[a] See footnotes to Table IV. [b] In each case the D_{4h} representation is e_u, while the molecular symmetry is C_{2v}, with y as the C_2 axis. The other component of the e_u mode has x as the C_2 axis; similar transition moments are generated, with x and y operators interchanged and MO 4 replacing 5.

tween the $^2B_1$ ground state and the $^2A_1$ state, while a 10° bend yields a moment of −0.135 A. These bends correspond to ligand displacements of 0.2025 and 0.405 A, respectively, so the ratio of the transition moment to the displacement is −0.333 in each case. The nuclear integral is merely a nuclear dipole matrix element between the vibrational states associated with the ground and excited electronic states, multiplied by this ratio, which we denote by $A(i, j, k)$ for electronic states i and k with the jth component of the electric dipole operator $\mathbf{R}$. The vibrational functions are harmonic oscillator functions using force constants taken from the LCAO–MO energy, $E_e(Q)$. If the force constants are essentially the same for ground and excited states, the usual vibrational selection rule $\Delta v = \pm 1$ governs the vibronic transition.

Tables IV and V show values of the ratio $A(i, j, k)$, together with computed force constants and vibrational frequencies[46] for all odd-parity modes of a tetragonally elongated $CuCl_6^{4-}$ complex. The oscillator strength

All *f* values represent the vibronic intensity at 0°K, with no thermally excited vibrations. The increase in the intensity with temperature can be easily derived from the detailed theory[48] worked out for the UCl_6^{2-} system.

Departures from simple harmonic oscillator vibrational selection rules will occur either if anharmonic terms are important or if the excited-state harmonic frequency differs from that for the ground electronic state. For the b_{2u} component of the t_{2u} bending mode, calculated frequencies (in cm^{-1}) are 105 ($^2A_{1g}$), 101

(46) The effective masses are $4m_{Cl}$ for the t_{2u} bend and $2m_{Cl}(1 + (2m_{Cl}/m_{Cu}))$ for the t_{1u} stretch. For the t_{1u} bend the mass is $4m_{Cl}(1 - (4m_{Cl}\cos^2\theta/MW))$, where θ is the bending angle (Table II) and MW is the molecular weight; $\cos^2\theta$ is taken to be unity for small deformations. For each mode the variable is the displacement of a ligand atom (Tables II, III) in centimeters.

(47) See ref 37, pp 41–57.

(48) R. A. Satten and E. Y. Wong, *J. Chem. Phys.*, **43**, 3025 (1965).

($^2B_{2g}$), and 91 (^2E_g), compared with the ground-state value of 120. For the a_{2u} component of the t_{1u} bend, the values for the same excited states are 195, 191, and 181, compared to 200 in the ground state, while for the a_{2u} component of the t_{1u} stretch, the values are 109, 191, and 121, compared to 216. Thus the excited-state odd-parity bending frequencies are nearly the same as their ground-state values, justifying the use of harmonic oscillator selection rules, while the odd-parity stretching frequency is computed to differ significantly for the $^2A_1$ and ^2E states from that for $^2B_{1g}$. However, it should be noted that the simple LCAO–MO method occasionally fails badly in describing asymmetric stretching modes, as found in studies[49] of XeF_2 and XeF_6, where negative force constants were obtained for such modes, so that the computed values of odd stretching frequencies for $CuCl_6^{4-}$ may not be meaningful in comparison to the bending frequencies.

Vibronic oscillator strengths computed with respect to the tetragonally compressed ground state, transforming like $3z^2 - r^2$, differ appreciably from the values in Tables IV and V for the elongated ground state. For example, the t_{2u} (b_{2u}) and t_{1u} (a_{2u}) bending modes induce oscillator strengths for the $^2A_{1g} \rightarrow {}^2E_g$ transition of about one-fourth the corresponding $^2B_{1g} \rightarrow {}^2E_g$ values in Table IV. In addition, some of the transition moments change sign, meaning that the parameter A is a complicated function of the stretching coordinate α, besides being an odd function of the odd-parity coordinate Q. Hence at temperatures where the α motion is essentially free, the total transition moment contains an α integration leading to complicated α-selection rules accompanying the vibronic transition.

In summary, the LCAO–MO method yields vibronic oscillator strengths for $CuCl_6^{4-}$ of the order of 10^{-4}, which is the frequently observed[50] magnitude of such strengths in transition metal complexes. It is not necessary to resort to the cumbersome procedure[42] of expanding the electronic wave function of the distorted molecule in the basis set of wave functions for the undistorted molecule. The striking feature is the polarization of the $^2B_{1g} \rightarrow {}^2B_{2g}$, ^2E_g transitions with the electric vector perpendicular to the fourfold axis of the complex. This polarization could possibly be detected even in a cubic lattice like NaCl, if the Cu(II) concentration were high enough, by observing the change in optical intensity upon application of uniaxial stress parallel to the (100) axis. From the epr spectrum of Cu(II) in NaCl it is known[8] that a stress of 1100 kg/cm^2 at 77°K reduces to one-fourth the population of that well having its symmetry axis parallel to the stress, while increasing the population of each of the other two wells to three-eighths.

Finally the intensity appears to arise in our scheme from the mixing of the even-parity 3d AO's both with the Cu(4p) AO's and with odd-parity[51] ligand symmetry MO's. For example, a 5° out-of-plane bend along the t_{2u} (b_{2u}) coordinate mixes Cu($4p_z$) into the mostly $x^2 - y^2$ MO with a coefficient of 0.032, adds Cl($3p_z$) from Cl atoms 3–6 (see Table II) with coefficients of -0.043 each, and Cl(3s) from Cl atoms 1 and 2 with coefficients of ± 0.023, respectively. Coefficients of other AO's in this MO are close to the values for the b_1 column of Table I, keeping in mind that for the distorted complex they are coefficients of displayed AO's.

Acknowledgments.—The author wishes to thank Dr. R. H. Borcherts for the suggestion of this problem and for permission to quote prior to publication details of the epr spectrum of Cu(II) in NaCl. The author also thanks Dr. A. W. Overhauser for invaluable discussions, especially of the Born–Oppenheimer approximation.

Appendix A
Possible Breakdown of the Born–Oppenheimer Approximation

Consider a total electronic–nuclear wave function $\Psi_{e,n}$ of the Born–Oppenheimer type (eq 1), with Q denoting α only. The electronic ground-state function $\psi_e(\alpha)$ is given by eq 9, while the corresponding Jahn–Teller half-state $\psi_e'(\alpha)$ is obtained by replacing $\cos(\alpha/2)$ with $-\sin(\alpha/2)$ and replacing $\sin(\alpha/2)$ with $\cos(\alpha/2)$. If the barrier height B is zero, the nuclear functions $\varphi_n(\alpha, m)$ and their energies are given by eq 10 and 11, respectively. If $\mathcal{H}$ is the total electronic–nuclear Hamiltonian,[52] then

$$\mathcal{H}\Psi_{e,n} = \mathcal{H}\psi_e\varphi_n = G\left[m^2\psi_e\varphi_n - 2\frac{\partial\psi_e}{\partial\alpha}\frac{\partial\varphi_n}{\partial\alpha} - \frac{\partial^2\psi_e}{\partial\alpha^2}\varphi_n\right] \tag{A1}$$

where G is the constant from eq 11. Since

$$\frac{\partial\psi_e}{\partial\alpha} = {}^1/_2\psi_e' \tag{A2}$$

and

$$\frac{\partial^2\psi_e}{\partial\alpha^2} = -{}^1/_4\psi_e \tag{A3}$$

then

$$\langle\psi_e\varphi_n(m)|\mathcal{H}|\psi_e\varphi_n(m)\rangle = (m^2 + {}^1/_4)G \tag{A4}$$

Thus there is a first-order correction of $G/4$ to the α-vibrational energy when the full Hamiltonian is used, doubling the zero-point energy in this zero-barrier limit from $G/4$ to $G/2$, or about 1.75–3.50 cm^{-1}.

The off-diagonal matrix element of $\mathcal{H}$ is a measure of the breakdown of the Born–Oppenheimer approximation and is

$$\langle\psi_e'\varphi_n(m)|\mathcal{H}|\psi_e\varphi_n(m)\rangle = -imG \tag{A5}$$

(49) L. L. Lohr, Jr., submitted for publication.

(50) For example, see O. Holmes and D. S. McClure, *J. Chem. Phys.*, **26**, 1686 (1957).

(51) Charge-transfer states of ^2E_u symmetry occur at the tetragonally elongated minimum with energies of 5.42, 5.80, and 6.51 ev, and with absorption intensities of 0.385, 0.483 × 10^{-2}, and 0.616, respectively, all for $\mathbf{E}\perp C_4$. Absorption to the $^2B_{2u}$ state at 5.75 ev is allowed for $\mathbf{E}\|C_4$, but the intensity is zero in the approximation of ref 45.

(52) J. C. Slater, "Quantum Theory of Molecules and Solids," Vol. I, McGraw-Hill Book Co., Inc., New York, N. Y., 1963, p 252.

If G is 7.05 cm^{-1}, this element has a magnitude of 3.50 cm^{-1} for $m = \pm 1/2$, negligible compared to the 1.17-ev or 9450-cm^{-1} difference in the diagonal electronic energies (Figure 2).

Now the electronic energies are not affected by multiplying $\psi_e(\alpha)$ and $\psi_e'(\alpha)$ by a phase factor $\exp(iF(\alpha))$, where $F(\alpha)$ must equal $k\alpha$ ($k = 0, \pm 1, \pm 2, \pm 3$, etc.) to satisfy the boundary condition that $\Psi_{e,n}(\alpha + 2\pi) = \Psi_{e,n}(\alpha)$. However, the first-order correction to the energy is now $(2mk + k^2 + 1/4)G$, making the total diagonal energy equal to $[(m + k)^2 + 1/4]G$. Thus the effective vibrational quantum number is $m + k$, and in fact the off-diagonal element (eq A5) becomes $-i(m + k)G$. While k can be chosen to make this matrix element arbitrarily large, no choice makes it zero, since k and m are integral and half-integral, respectively. Both the first- and second-order corrections to the α energy of six-coordinated Cu(II) are minimized by the initially obvious phase choice of $k = 0$. It would be very interesting to find a molecule in which the simplest choice of phase for $\psi_e(Q)$ was not the best, or else to prove this impossible in general.

Consider now the periodic potential (eq 4), assuming that B is the same for both ground and excited electronic states. For simplicity let φ_n be confined to a single well (eq 12). Although the first-order correction to the α energy is the same as when B is zero, the off-diagonal element analogous to eq A5 is $(c/2)^{1/2}G$, compared to the zero-point nuclear kinetic energy of $(c/2)G$, where c is given by eq 13. For B and G of 300 and 7.05 cm^{-1}, respectively, the off-diagonal element equals 15.5 cm^{-1}, a sizable increase over the 3.5-cm^{-1} value when B is zero. The excited-state $\Psi_{e,n}'$ mixed into the $v = 0$ ground state by this element contains the $v = 1$ vibrational state, so that v, unlike m in the zero-barrier limit, is no longer a good quantum number when the correction terms of eq A1 are considered.

If the more reasonable assumption is made that B in the excited state differs both in sign and magnitude from the ground-state value, the harmonic approximation to the excited state yields vibrational functions $\varphi_n'(\alpha)$ centered about $\alpha = \pm\pi/3$ and with a different c value. Again off-diagonal elements like eq A5 may be derived, requiring overlap integrals between $\varphi_n'(v')$ and $\partial\varphi_n(v)/\partial\alpha$.

Appendix B
Uniaxial Stress Perturbations of Cu(II) in NaCl

Epr studies[7,8] of Cu(II) in NaCl at 77.4°K have shown that the application of a uniaxial stress of 1100 kg/cm^2, or 1.08×10^9 $dynes/cm^2$, in a direction parallel to a C_4 crystal axis decreases to one-fourth the fraction of complexes having their tetragonal axes parallel to the stress, while increasing to three-eighths the fraction with their axes in each of the two directions perpendicular to the stress. Any changes in the g values with stress were too small to be detected.

The changes in the populations of the three wells represent a perturbation of the nuclear potential energy (eq 4) and can be calculated by the LCAO–MO method as a function of stress-induced displacements of the Cl nuclei in a $CuCl_6^{4-}$ complex. Assuming that these displacements are given by the NaCl elastic constants[53] of $S_{11} = 2.29 \times 10^{-12}$ and $S_{12} = -0.465 \times 10^{-12}$ $cm^2/dyne$, stress parallel to C_4 of a tetragonally elongated complex reduces the axial bond length by 0.0063 A from 2.55 A, while increasing the equatorial length by 0.0012 A from 2.325 A. Similar displacements are obtained for stress perpendicular to C_4 of the elongated complex, and for stress parallel and perpendicular to C_4 of the compressed complex having axial and equatorial bond lengths of 2.25 and 2.475 A, respectively. The corresponding energy changes are shown in Figure 7 for stress parallel to y, together with a plot of $V(\alpha)$ for zero stress. In addition to an upward shift of 0.027 ev for all configurations, the Y structure is raised in energy by 0.006 ev relative to X and Z, while X' and Z' are raised by the same amount relative to Y' (see caption for Figure 4). Using the energy difference of 0.006 ev, or 47 cm^{-1}, between Y and X or Z, the populations of the three wells at 77.4°K are 0.170, 0.415, and 0.415. An energy difference of only 22 cm^{-1} is required to fit the observed values, so the computed difference is about twice too large.

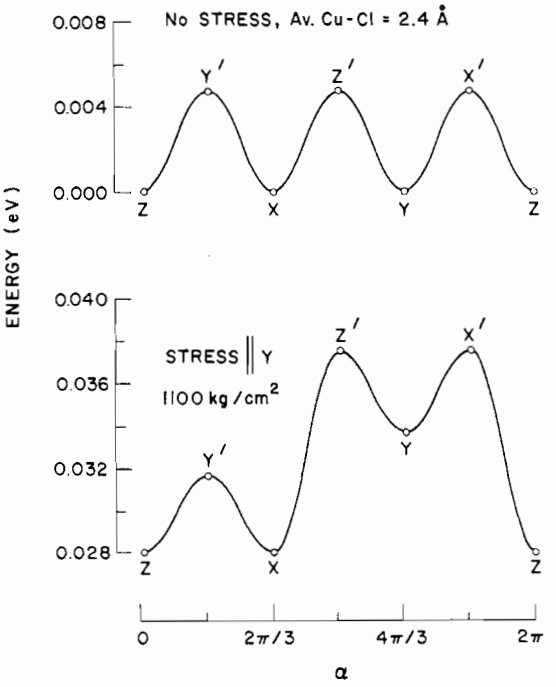

Figure 7.—The nuclear potential $V(\alpha)$ without stress (upper curve) and with a uniaxial stress of 1100 kg/cm^2 parallel to a C_4 axis of NaCl. See legend for Figure 4 for explanation of the letters X, X', etc. All energies are total MO energies relative to that for the elongated minimum of Figure 2.

It is important to check that the model does not predict large g-value changes. Five values were computed, $\Delta g_z/\Delta z$, $\Delta g_z/\Delta x$, $\Delta g_x/\Delta x$, $\Delta g_x/\Delta y$, and $\Delta g_x/\Delta z$, where Δx, Δy, and Δz denote stresses parallel to these

(53) J. K. Galt, *Phys. Rev.*, **73**, 1460 (1948); values tabulated by H. B. Huntington, *Solid State Phys.*, **7**, 213 (1958).

axes. The largest change is -0.005 for $\Delta g_z/\Delta x$, while $\Delta g_z/\Delta z$ is 0.000. Since g_z depends on the splitting between the MO's that are largely $3d(x^2 - y^2)$ and $3d(xy)$ AO's, respectively (see section on Spin–Orbit Coupling and g Values), a stress parallel to z has little effect, while a stress parallel to x raises the $^2B_{2g}$ excited state (see eq 6), having two electrons in the mostly-$3d(x^2 - y^2)$ MO, relative to the ground state, having only one, thus decreasing g_z. The experimental uncertainty[7,8] on g_z (or $g_{||}$) is ± 0.01, so a change of -0.005 would not be detectable.

A similar analysis shows that if the tetragonally compressed structure for $CuCl_6^{4-}$ were lower in energy than the elongated structure (negative α barrier), then two minima would be raised in energy by stress, rather than one as is observed. In each case, stress primarily raises in energy the MO containing the Cu AO with its charge density concentrated along the axis parallel to the stress. The total states respond to the stress in accord with occupation numbers of 1 or 2 for the most strongly affected MO. Hence a compressed structure with its C_4 axis parallel to the stress is less affected than one with C_4 perpendicular to the stress, since the former has only one electron in the mostly-$3d(3z^2 - r^2)$ MO, while the latter has two in the mostly-$3d(z^2 - x^2$ or $z^2 - y^2)$ MO (the relative position of Y' relative to X' and Z' in Figure 7 holds even for negative barrier). Thus the stress-induced population changes provide an independent confirmation of the positive sign of the α barrier (eq 4) in $CuCl_6^{4-}$.

CONTRIBUTION FROM THE CHEMISTRY DEPARTMENT,
THE UNIVERSITY OF WESTERN ONTARIO, LONDON, CANADA

The Reaction of Hexafluoroacetone with Silanes. II. Possible Ionic Intermediates[1]

BY A. F. JANZEN AND C. J. WILLIS

Received March 20, 1967

The mechanism of the reaction of hexafluoroacetone with trimethylsilane has been reconsidered in the light of results now available on other reactions involving nucleophilic attack on hexafluoroacetone; these include the reaction of the ketone with alkyl halides in the presence of sodium and the reaction of hexafluoroacetone with tertiary amines. It is now thought probable that the initial reaction of a silane with hexafluoroacetone is a hydride abstraction, giving a fluorinated alkoxide ion. Claims that hexafluoroacetone forms complexes with compounds of group IV elements are reexamined, and it is concluded that present evidence does not support such a suggestion.

The addition reactions of hexafluoroacetone across Si–H bonds have received attention recently. We have reported[2] the reaction of the ketone under free-radical conditions with methyl-, dimethyl-, trimethyl-, or trichlorosilane to give a variety of hexafluoroisopropoxysilanes containing the grouping $SiOCH(CF_3)_2$. Under ionic conditions (dark, liquid phase, 20° or below) only trimethylsilane reacted, the products being the 1:1 adduct, $(CH_3)_3SiOCH(CF_3)_2$, and a smaller yield of the 2:1 adduct, $(CH_3)_3SiOC(CF_3)_2OCH(CF_3)_2$.

In a paper appearing at the same time as ours, Cullen and Styan[3] described similar work on the reaction of hexafluoroacetone with trimethylsilane, -germane, and -stannane and with dimethylstannane. In each case, they reported ready formation of the hexafluoroisopropoxides. However, they did not find the 2:1 adduct of hexafluoroacetone with trimethylsilane mentioned above, but reported instead an unstable adduct, $(CH_3)_3SiOCH(CF_3)_2 \cdot (CF_3)_2CO$, dissociating readily at 20° to $(CH_3)_3SiOCH(CF_3)_2$ and hexafluoroacetone. They point out in a footnote that this would appear to be a different species from our 2:1 adduct, which is stable indefinitely at 20° and may be distilled repeatedly without dissociation at its normal boiling point of 135°. However, evidence from nuclear magnetic resonance spectra, discussed below, suggests that this point may be questioned.

In the papers referred to above, both Cullen and Styan and ourselves suggested that the mechanism of the liquid-phase reactions of hexafluoroacetone with group IV hydrides involved as a first step the nucleophilic attack of the carbonyl oxygen on the central metal or metalloid atom, giving a five-coordinate intermediate. The hexafluoroisopropoxides were then formed by intermolecular hydride transfer.

Fresh evidence now available leads us to reject the above process in favor of an ionic mechanism in which the first step is the abstraction of a hydride ion by hexafluoroacetone, giving a hexafluoroisopropoxide ion, $HC(CF_3)_2O^-$.

Experimental Section

General techniques have been described previously,[2] as has the reaction of hexafluoroacetone with trimethylsilane. Nuclear magnetic resonance spectra were recorded on Varian Model A-60 and DP-60 instruments using 60 Mcps. Chemical shifts are relative to internal TMS, unless otherwise stated.

(1) Presented in part at the 49th Conference of the Chemical Institute of Canada, Saskatoon, June 1966. Reference 2 is regarded as part I.
(2) A. F. Janzen and C. J. Willis, *Can. J. Chem.*, **43**, 3063 (1965).
(3) W. R. Cullen and G. E. Styan, *Inorg. Chem.*, **4**, 1437 (1965).